
This is an electronic reprint of the original article.
This reprint may differ from the original in pagination and typographic detail.

Chu, Guang; Sohrabi, Fereshteh; Timonen, Jaakko V.I.; Rojas, Orlando J.

Dispersing swimming microalgae in self-assembled nanocellulose suspension: Unveiling living colloid dynamics in cholesteric liquid crystals

Published in:
Journal of Colloid and Interface Science

DOI:
[10.1016/j.jcis.2022.05.012](https://doi.org/10.1016/j.jcis.2022.05.012)

Published: 15/09/2022

Document Version
Publisher's PDF, also known as Version of record

Published under the following license:
CC BY

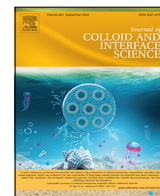
Please cite the original version:
Chu, G., Sohrabi, F., Timonen, J. V. I., & Rojas, O. J. (2022). Dispersing swimming microalgae in self-assembled nanocellulose suspension: Unveiling living colloid dynamics in cholesteric liquid crystals. *Journal of Colloid and Interface Science*, 622, 978-985. <https://doi.org/10.1016/j.jcis.2022.05.012>

This material is protected by copyright and other intellectual property rights, and duplication or sale of all or part of any of the repository collections is not permitted, except that material may be duplicated by you for your research use or educational purposes in electronic or print form. You must obtain permission for any other use. Electronic or print copies may not be offered, whether for sale or otherwise to anyone who is not an authorised user.



Contents lists available at ScienceDirect

Journal of Colloid and Interface Science

journal homepage: www.elsevier.com/locate/jcis

Dispersing swimming microalgae in self-assembled nanocellulose suspension: Unveiling living colloid dynamics in cholesteric liquid crystals

Guang Chu^{a,*}, Fereshteh Sohrabi^b, Jaakko V.I. Timonen^b, Orlando J. Rojas^{a,c,*}^a Department of Bioproducts and Biosystems, Aalto University School of Chemical Engineering, Vuorimiehentie 1, 02510 Espoo, Finland^b Department of Applied Physics, Aalto University School of Science, Puumiehenkuja 2, 02150 Espoo, Finland^c Bioproducts Institute, Department of Chemical & Biological Engineering, Department of Chemistry and Department of Wood Science, 2360 East Mall, The University of British Columbia, Vancouver, BC V6T 1Z3, Canada

GRAPHICAL ABSTRACT

A new hybrid soft matter was realized by the combination of nontoxic cholesteric liquid crystal dispersed living microalgae, displaying nonequilibrium swimming behavior of microalgae and hydrodynamic fluctuations in local liquid crystal medium.

G.C. prepared the hybrid liquid crystal dispersed self-propelled colloids and carried out the experimental measurement and data analysis. F.S. and J.T. prepared the living microalgae. G.C. designed and led the project. Discussions and manuscript drafting involved the contributions of all authors. All authors have given approval to the final version of the manuscript.



ARTICLE INFO

Article history:

Received 16 February 2022

Revised 13 April 2022

Accepted 2 May 2022

Available online 05 May 2022

Keywords:

Nanocellulose

Liquid crystal

Living colloids

Active matter

Dynamic assembly

ABSTRACT

Active matter comprises individual energy-consuming components that convert locally stored energy into mechanical motion. Among these, liquid crystal dispersed self-propelled colloids have displayed fascinating dynamic effects and nonequilibrium behaviors. In this work, we introduce a new type of active soft matter based on swimming microalgae and lyotropic nanocellulose liquid crystal. Cellulose is a kind of biocompatible polysaccharide that nontoxic to living biological colloids. In contrast to microalgae locomotion in isotropic and low viscosity media, we demonstrate that the propulsion force of swimming microalgae can overcome the stabilizing elastic force in cholesteric nanocellulose liquid crystal, with the displacement dynamics (gait, direction, frequency, and speed) be altered by the surrounding medium. Simultaneously, the active stress and shear flow exerted by swimming microalgae can introduce local perturbation in surrounding liquid crystal orientation order. The latter effect yields hydrodynamic fluctuations in bulk phase as well as layer undulations, helicoidal axis splay deformation and director bending in the cholesteric assembly, which finally followed by a recovery according to the inherent

* Corresponding authors.

E-mail addresses: chuguang88@gmail.com (G. Chu), orlando.rojas@aalto.fi, orlando.roja@ubc.ca (O.J. Rojas).<https://doi.org/10.1016/j.jcis.2022.05.012>

0021-9797/© 2022 The Authors. Published by Elsevier Inc.

This is an open access article under the CC BY license (<http://creativecommons.org/licenses/by/4.0/>).

viscoelasticity of liquid crystal matrix. Our results point to an unorthodox design concept to generate a new type of hybrid soft matter that combines nontoxic cholesteric liquid crystal and active particles, which are expected to open opportunities in biosensing and biomechanical applications.

© 2022 The Authors. Published by Elsevier Inc. This is an open access article under the CC BY license (<http://creativecommons.org/licenses/by/4.0/>).

1. Introduction

Active matter is driven by internal sources of energy, which universally exists in nature and permeates to a broad range of length scales, ranging from macroscopic schools of fish to micro/nanoscale cells and molecular motors [1]. Owing to long-range hydrodynamic and short-range excluded volume effects, the motile components in active matter can generate mechanical stress and flow within the fluid, thereby producing complex inter-particle and particle-medium interactions [2]. The internally injected energy drives the system out of equilibrium and lead to unique collective behavior and beautiful pattern formation. Natural active particles, e.g., bacteria and microalgae, adapt to a rich variety of microenvironments and display a distinct ability to sense and navigate in search of nutrients following local mechanical motion. Most microorganisms inhabit isotropic Newtonian fluids and possess direction-independent physical properties [3]. By contrast, some specialized cases have shown the ability to colonize anisotropic media and display direction-dependent collective migration [4]. Therefore, understanding how the environmental anisotropy influences the dynamic behavior of biological particles and *vice-versa*, presents a fertile field relevant to soft matter research.

Liquid crystals (LCs) are anisotropic fluids that preserve long-range orientational order and flowing mobility, have been widely used as reconfigurable soft matter systems to sense the external stimuli in local environments [5–7]. Dispersing micrometer-sized guest colloidal particles into LC can lead to complex particle assemblies as well as distortions and topological defects in the surrounding environment, revealing an anisotropy-induced interplay between guest particles and the host medium [8–10]. While LC-mediated self-assembly of static colloids is a well-established phenomenon, much less is known about the dynamic behavior of active particles dispersed in LC media. Interestingly, using nontoxic LC as the culturing medium allows the preservation of orientational order of LC phase as well as swimming ability of active biological particles, integrating into living hybrid liquid crystal colloids that combine the anisotropic behavior of fluid phase with microorganism swimming activity [11,12]. Surface-active micellar and thermotropic LCs are usually toxic to biological cells, while certain types of lyotropic LCs exhibit much lower toxicity [13]. Recently, several studies have reported on given types of bacteria that survive and swim in aqueous solutions of disodium chromoglycate [14], polymers [15] or DNA molecules [16] with nematic LC phase. However, to the best of our knowledge, no attempt has yet been made to develop a more complex hybrid colloidal system, specifically, controlled cholesteric LC phase with swimming microalgae. Unlike the swimming behavior of rod-like bacteria, ellipsoidal microalgae can create volume-induced distortions in surrounding fluid medium and generate oscillatory flow during the flagella beating process [17], introducing local perturbations to the LC orientational order both in terms of the helicoidal axis and degree of order, therefore provide more information on the dynamic mesostructure than simply nematic LC medium.

Cellulose is perfectly in line with the above requirements. Cellulose is linear chain polysaccharide composed of D-glucose subunits. As an important part of the ecosystem, many microorganisms in nature can digest and harvest energy from cellulose or produce cellulose as the cytoderm building blocks [18].

These observations place cellulose as an inherently nontoxic construct. When bulk cellulose fibrils are subjected to controlled acid hydrolysis, the less ordered regions of the microfibrils can be clipped and yield polydispersed crystalline nanorods, dubbed as cellulose nanocrystals (CNCs) [19–21]. CNCs preserve the biocompatibility features of the precursor material and demonstrate promising prospects not only for biomedical applications, but also as an ideal component of controlled particle self-assembly [22]. While aqueous CNCs suspension can spontaneously form into a lyotropic cholesteric LC phase above a critical concentration with the nanorods self-assembled locally uniform along a common direction [23], acting as a robust LC platform for soft matter research. Compared with the nematic counterpart, previous reports demonstrate more complex behaviors and emerging applications for cholesteric LC [24–26]. Up to now, numerous studies on CNC-derived cholesteric LC have been focused on photonics [27–30], templating [31–33], controlled self-assembly [34–37], and chirality aspects [38–40], however, the potential capacity to utilize cellulose biocompatibility, for instance, to host living biological cells remains as an unexplored subject. Breaking apart from current cellulose research is an attractive proposition. A reasonable inquiry is to develop a new class of LC-dispersed colloids that consist of nontoxic cholesteric CNC and living self-propelled particles with controllable dynamic affects and nonequilibrium behaviors.

In this work, we present a study of motile *Chlamydomonas reinhardtii* (CR) cells motion in aqueous CNC suspension with long-range cholesteric LC ordering. The swimming activity of the microalgae is preserved in the presence of CNC particles and can be further extended to nontoxic LC environments revealing the excellent biocompatibility with CR. We find that the suspended CR can overcome the stabilizing elastic force inherent to cholesteric LC medium, yielding a strong coupling between LC orientational order and CR activity. Such effects alter not only the CR swimming dynamics but also the surrounding long range fingerprint texture. Compared with isotropic environment, the swimming gait, direction, and speed of CR in cholesteric CNC medium can be manipulated by the LC anisotropy, given varying apparent viscosities along different pathways. During the swimming process, the beating flagella together with the micrometer-sized prolate cell body, perturb the director of local helical order with pitch undulation and helicoidal axis splay deformation, generating large scale hydrodynamic fluctuations in surrounding cholesteric LC medium with a length scale that balances CR activity and make the flagella beating process birefringent visible. Owing to the inherent viscoelasticity of the LC medium, the distortions and instability in surrounding cholesteric LC eventually return to its initial state as the CR swims away. Hence, the dynamic behavior of swimming CR microalgae and orientational order of cholesteric LC medium are coupled to each other, leading to a hybrid living LC system that may have intriguing applications in various fields.

2. Experimental section

2.1. Materials and apparatus

All Chemicals were used as received without further purification. Cellulose nanocrystal (CNC) gel (10 wt%) was obtained from the U.S. Forest Products Laboratory at University of Maine. The

CNC was prepared by sulfuric acid hydrolysis of wood fibers. After dilution and membrane filtration, the resulting system consisted of a concentrated suspension of CNC that had typical dimensions of ~ 10 – 15 nm in width and ~ 300 – 400 nm in length and contained 0.95 wt% sulfur. Dextran (from *Leuconostoc mesenteroides*, $M_w = 9000$ – 11000) was purchased from Sigma Aldrich. De-ionized water was obtained from the Millipore-purified water system.

Polarized optical microscopy (POM) characterization was conducted on Olympus BX53-P microscope with images taken by polarizers in a perpendicular arrangement to verify the anisotropy of the samples. Videos were taken by the same microscope with a motorized stage, and a high-resolution DP74 camera (Olympus, resolution of 5760×3600 pixels) were used to record the motion of individual living cells in suspension. Images were acquired with the frame rate up to 50 frames/s, at $200 \times$ magnification in cross-polarized light. The acquired videos were converted into image sequences and processed in imageJ software to create cell trajectory. The cell velocity was determined by combining the position of the cell at each interval in a cell track with the CCD frame rate. Discovery DHR-2 rotational rheometer (TA Instruments, USA) was used to characterize the rheological properties of the suspension under steady-state shear flow. All rheological measurements were performed at room temperature (25 °C).

2.2. *Chlamydomonas reinhardtii* (CR) cell culture

The axenic cultures of *Chlamydomonas reinhardtii* strain CC125, and Sueoka high salt medium used for cultivation was obtained from the Chlamydomonas Resource Center (Department of Plant and Microbial Biology, University of Minnesota) [41]. The liquid cultures were kept on an orbital shaker (Grant-bio PSU-10i) in an incubator (thermo-statically controlled incubator, Lovibond) at 27 °C on a 12 h/12 h bright/dark light cycle to optimize cell size and motility synchronization. The illumination was carried out with a cold white light LED panel with constant flux of 30 W/m². To optimize aeration, the containers were connected to silicon tubings (Fisherbrand, Silicon Platinum-cured Tubing 11502573, diameter 9 mm) connected to sterile filters (Fisherbrand, Sterile PES 15206869), so that the CR cells have proper access to ambient air (and CO₂ required for photosynthesis), and to avoid suffocation of cells from excess oxygen produced during their photosynthesis. To compensate the evaporated water, a bottle of Milli-Q water was connected to the container of liquid culture, and to enhance the aeration, an air pump (aquarium mouse air pump M101) was connected to the water bottle. The cultures were renewed once a week by diluting in HS medium at a ratio of 1:100, and the experiments were carried out 3–4 days after renewing the cultures.

2.3. Preparation of CNC suspension

In a typical experiment, CNC suspensions with varying concentration (0.5, 3.5, 6.0 wt%) were prepared by diluting the initial CNC gel (10 wt%) with de-ionized water. A small amount of dextran (0.1 wt%) was added into the suspension to make it more suitable for cell culture. All of the suspensions were sonicated for 2 min at the power input of 50% (VCX-750, Sonics & Materials, Inc) and preserved in glass vials for further usage. There occurred a phase separation for CNC suspension of 3.5 wt% and 6.0 wt% after standing for two days, whereas the CNC suspension with low concentration (0.5 wt%) kept totally isotropic. Aqueous CNC cholesteric liquid crystal was prepared by pipette removing the upper isotropic phase of 6.0 wt% CNC suspension with bottom phase termed as the anisotropic phase.

2.4. Preparation of LC dispersed swimming CR

Firstly, the living CR cells in water were concentrated by centrifugation for 5 min at 700g to remove the upper supernatant. Then the purified CR cells were redispersed in the as-prepared CNC cholesteric liquid crystal phase with the final concentration of 10^2 cells/mL. At this concentration, CNC can self-assemble into helical cholesteric phase without disturbing the CR moving activity. After that, a small volume of CNC-CR solution was subsequently sandwiched between the two rubbed hydrophilic glass substrates to ensure the directional alignment and planar anchoring of CNC [42], and finally sealing with adhesive spacer (Memcon) in a cavity of 100 μ m.

3. Results and discussion

The first step in understanding LC dispersed self-propelled microalgae is to investigate the CR-fluid interactions in different environments. To ensure uniform size and motility, the CR we used was cultured in minimal media, on a 12 h bright /12 h dark light cycle and redispersed in pure water through centrifugation for further use (see Supporting Information). CR is unicellular photosynthetic microalgae with a roughly prolate cell body that is 10 μ m in diameter and swims with two long anterior flagella (Fig. 1a). As such, the flagella with microscopic hair-like structures, are heavily involved in the locomotion of the cells. The two flagella, usually 12 μ m in length and 300 nm in diameter, act as a pair, are termed as *cis* and *trans* due to their positions relative to the eyespot [43]. They perform cyclical breaststroke-like swimming style with unequal power and recovery strokes to generate propulsion, corresponds to an idealized ‘puller’ with far-field disturbance flow [44]. During the power stroke, the flagella extend upward and pull away from the body with the flagellar tips move in opposite directions, meanwhile the beating direction is immediately reversed during each subsequent recovery stroke [2]. As the host continuous medium, the colloidal nanocellulose suspension presents an excellent biocompatibility to living cells, including green microalgae. Before transfer CR into CNC suspension, a small amount of polysaccharose (dextran, 0.1 wt%) was added as nutrient without harming the cells and disturbing CNC self-assembly, which can be used to keep CR moving activity during a relatively long periods of time. The cell-cell and cell-CNC interactions are expected to be insignificant when the CNC concentration is low with a small amount of swimming CR (0.5 wt% for CNC and 10^2 cells/mL). In this condition, the obtained CNC suspension exhibited a Newtonian fluid behavior with the suspended CNC nanorods remain in an isotropic state (Fig. S1 and Movie S1, S2). The CR flagella synchronously beat at a frequency of ~ 50 Hz and propelled the cell body in an oscillatory manner, at a speed of 100 – 200 μ m/s along a random walk, similar to the CR swimming behavior in pure water (Fig. 1b and Movie S3, S4).

At an increased CNC concentration to 3.5 wt%, the suspension became viscoelastic and microscopic LC tactoid domains were formed, which owing to the lyotropic nature of CNC derived cholesteric LC (Fig. S2). Compared to the CR swimming behavior at low CNC suspension concentration, the fluid viscosity at high concentrations significantly modifies the beating pattern, frequency, and swimming speed. More specifically, both the beating frequency and swimming speed were hindered (as much as 90%) at an increased viscosity, an effect that is explained by the increase in fluid elastic stress between swimming CR (Fig. 1c). As far as the beating flagella, they were more mobile and bent over the whole cycle in the isotropic CNC suspension. By contrast, the beating pattern was severely restricted in the viscoelastic LC domains, similar to the behavior observed in concentrated polymer solutions

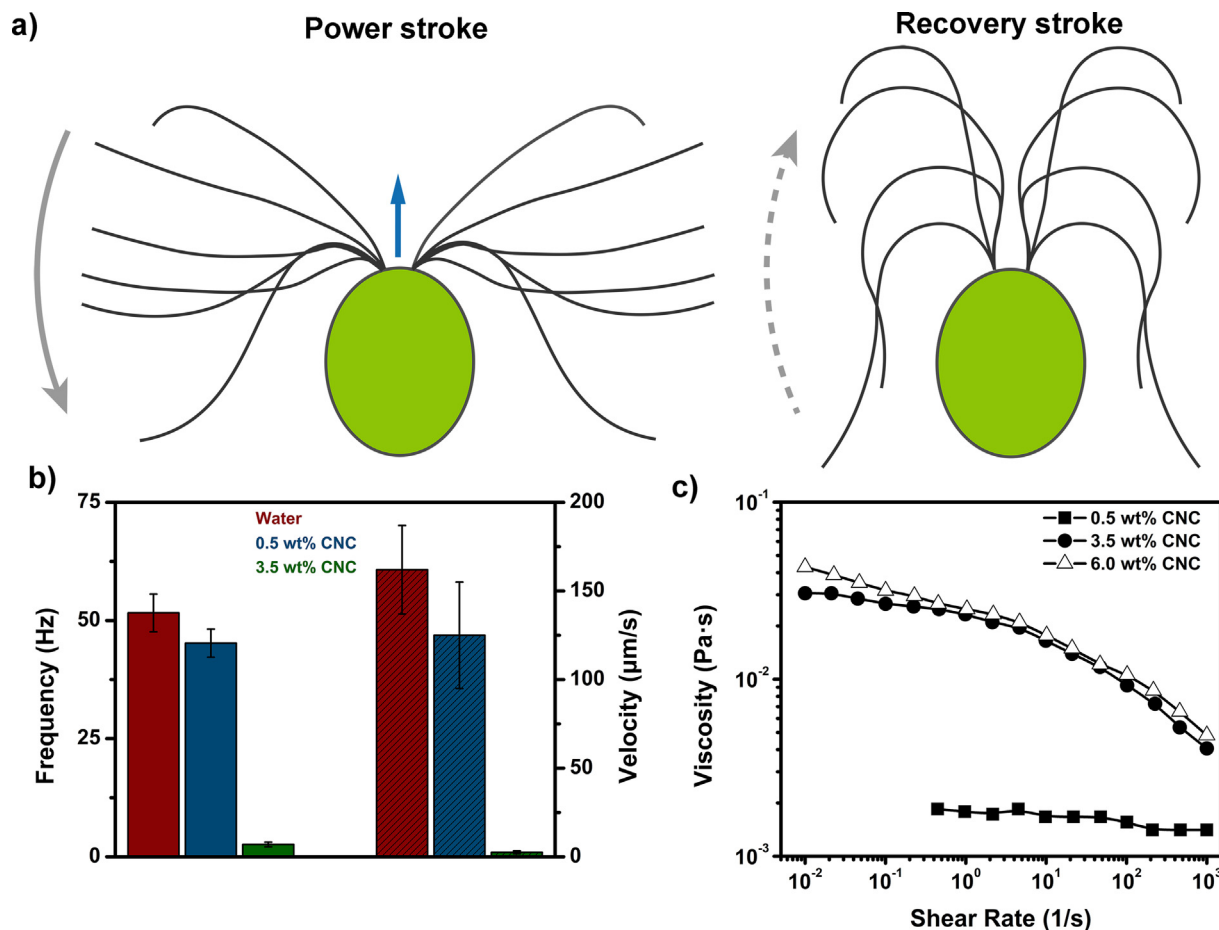


Fig. 1. (a) Schematic illustration of the movement of the CR flagella during a beat sequence that can be divided into power and recovery strokes, respectively. The beating flagella first moved backward (grey arrow) with the active forces exerted by surrounding fluid push the CR body forward (blue arrow), then the flagella recovered back to its initial position (dashed grey arrow) to complete the stroke cycle. (b) The beating frequency and moving velocity of CR dispersed in pure water, dilute 0.5 wt% CNC suspension and more concentrated 3.5 wt% CNC suspension. (c) Evolution of shear viscosity with shear rate at different CNC concentrations, showing a Newtonian fluid behavior at low CNC concentration and non-Newtonian one when LC domains were formed. (For interpretation of the references to colour in this figure legend, the reader is referred to the web version of this article.)

[45]. In the latter case, the movement was easily varied between synchronous and asynchronous beating patterns that pushed the cell body forward and distributed sharp turns, creating a run-and-tumble motion (Movie S5) [46]. Taking all together, these results revealed that the swimming activity of CR at low CNC concentrations remained unchanged compared to that of the aqueous background solution, whereas increasing the concentration of CNC led to the increase of viscosity in surrounding environment and further changed the swimming gait, speed and beating frequency.

The anisotropy character leads to numerous mechanisms by which colloidal particles move in a LC environment [47]. To connect the swimming activity of CR to its surrounding LC environment, we analyzed the locomotion trajectory and speed of CR in different regions. At high enough surrounding viscosity, many types of microorganism are unable to generate sufficient propulsion to move through the fluids [3]. In contrast, compared with the random moving path in isotropic medium, the motile ability of CR across varying regions is not significantly affected owing to the run-and-tumble motion. In principle, the swimming CR prefers to inhabit the easy pathway with the least resistance and low local viscosity to move across the anisotropic LC region. When the CNC concentration is increased to 3.5 wt%, the CNC suspension approaches a biphasic region in which the isotropic and cholesteric tactoid phases coexist. As the phase transition continues, neighbor-

ing cholesteric tactoids merge into a large area of cholesteric LC phase with the formation of typical fingerprint texture, implying the CNC orientation is homeotropically anchored, whereas the axis of the cholesteric helix lies parallel to the interface. As shown in Fig. 2a, an individual CR is seen to swim at varying velocities along a random path across the as-merged cholesteric LC phase into the isotropic area (Movie S6). The speed acquired in different regions by the swimming CR is set by the balance between internally driven propulsion forces and the Stokes drag force ($F_p = F_s = 6\pi\gamma Rv$, where v is the velocity, R is the radius and γ is the local viscosity) that corresponding to the surrounding medium.[48] The propulsion force can be estimated by measuring the CR velocity in the CNC suspension with pure isotropic state (0.5 wt%) due to its Newtonian behavior ($F_p \sim 10^{-11} \text{N}$). In the vicinity of cholesteric LC phase, the transient swimming velocity of CR is much smaller than the velocity measured in the cholesteric-isotropic boundary and the isotropic phase (Fig. 2b and Fig. S3), implying the non-homogeneous distribution of local viscosity in the different regions. By using video microscopy coupled with particle tracking routines, we estimated the apparent viscosity experienced by the motile CR suspended in cholesteric CNC phase to be $\gamma \sim 0.1 \text{ Pa}\cdot\text{s}$ (Supporting Information), which is slightly larger than the fluid viscosity in pure cholesteric ordered CNC suspension ($\gamma \sim 0.04 \text{ Pa}\cdot\text{s}$). These results indicate that the CR swimming activity has a

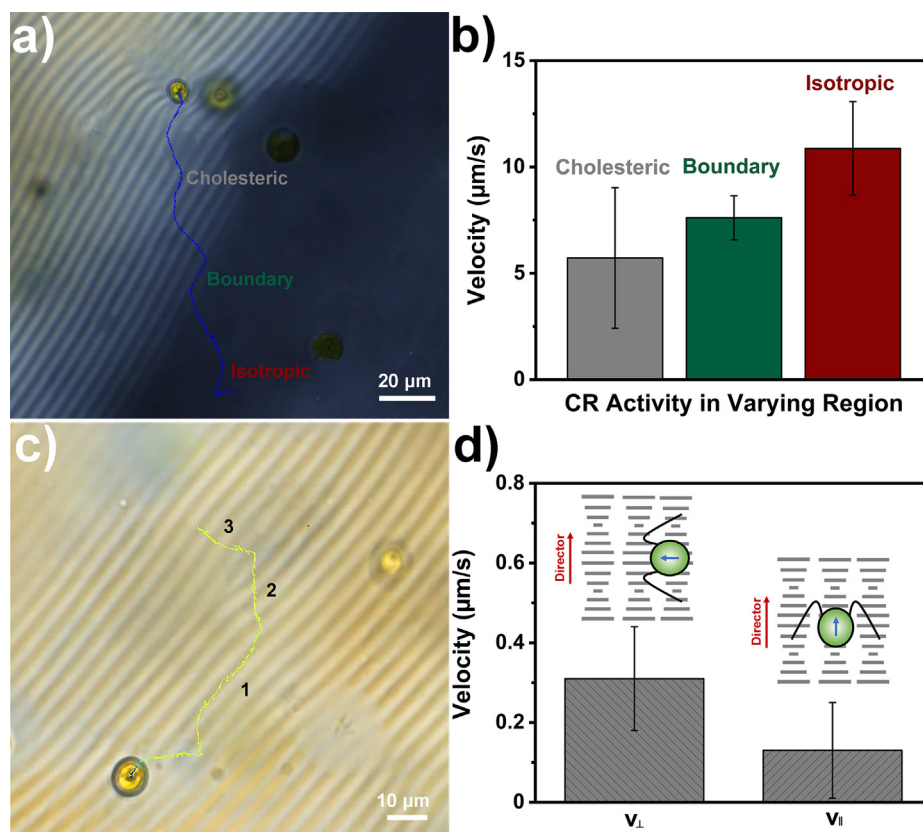


Fig. 2. Tracking CR swimming CR in varying given LC environments. (a) The moving trajectory of an active CR moving from the cholesteric LC region to the isotropic one and recorded during 30 s. (b) The swimming activity of CR in different regions that display a varying moving velocity. (c) The CR microswimmer in a large-area oriented cholesteric LC phase with the moving direction parallel (1), titled (2) and perpendicular (3) to the long-range ordered fingerprint texture. (d) Correlation between the direction of velocity and local helicoidal axis of cholesteric LC medium either perpendicular or parallel to each other.

fascinating effect on the viscosity of surrounding medium, namely, enhancing the shear viscosity, which is characteristic for puller-like swimmer kinematics [45].

In addition to the LC boundary, CR swimming in the bulk cholesteric region displayed an anisotropic activity character with varying self-propelled velocities. The orientation of CNC particles can be controlled by directional rubbing two hydrophilic glass slides or applying external magnetic field to align the cholesteric self-assembly. Fig. 2c and Movie S7 focus on the swimming behavior of CR in the bulk cholesteric medium and track the displacements with the motion trajectories, either parallel or perpendicular to the helicoidal axis of cholesteric phase. When the CR swimming direction was perpendicular to the helicoidal axis, that is, parallel to the stripes in fingerprint texture, the measured velocity $v_{\perp} = 0.31 \mu\text{m/s}$. In contrast, a much lower velocity was measured as $v_{\parallel} = 0.13 \mu\text{m/s}$ when moving in the direction parallel to the helicoidal axis but perpendicular to the stripes (Fig. 2d). Owing to the balance between propulsion and Stokes drag forces, the obtained anisotropic motile activity of CR in cholesteric LC phase implied the local orientation dependent viscosity difference ($\gamma_{\perp} < \gamma_{\parallel}$), where the CNC orientation order and elastic force around the moving CR particle couple with the moving direction. The obtained swimming CR derived microrheology studies have shown that the anisotropic viscoelastic properties of the LC medium are highly dependent on the helix orientation vector with respect to the moving direction, a remarkable increase in the viscosity arises when the cholesteric helix is oriented along the velocity direction which owing to the permeative effect in cholesteric LC [49,50]. Except for elastic stabilizing force between CR and LC medium,

the dispersed active CR also disturbed the local cholesteric CNC assembly during the swimming process. Compared with the moving direction that parallel to the director, it is easier for biased moving with the direction perpendicular to the helicoidal axis to splay the cholesteric CNC assembly rather than destroy it, resulting in the anisotropy in apparent viscosity [14].

Apart from the particle-LC interaction, when an active CR swims across a large area of LC environment, the resulting beating flagella induced flow can interact with the local LC medium to modify the local CNC orientational order with varying degrees of instabilities. Fig. 3a and Movie S8 exhibit the swimming process of active CR in a cholesteric LC matrix with large-area, oriented fingerprint texture. Compared with the CR trapped in a defect region, the swimming trajectory of CR in defect-free cholesteric region corresponded to a random walk due to the run-and-tumble motion with the average speed of $0.156 \mu\text{m/s}$ (Fig. S4), much smaller than that in an isotropic medium. This can be ascribed to the dramatic increase of LC viscosity. The bright and dark stripes in fingerprint textures became unstable when CR moved across, which was due to the flow induced layer undulations and hydrodynamic fluctuations in surrounding cholesteric LC medium (Fig. 3b). Besides, we also quantified the influence of active flow on CNC assembly through measuring the pitch undulations in cholesteric matrix with varying distances between moving CR. These results showed that the helical pitch perturbation intensity fell off in strength with twice the diameter of CR, whereas the flow-induced pitch undulation was suppressed beyond a certain range (Fig. 3c). Therefore, we can conclude that the obtained active flow generated by swimming CR is sufficiently

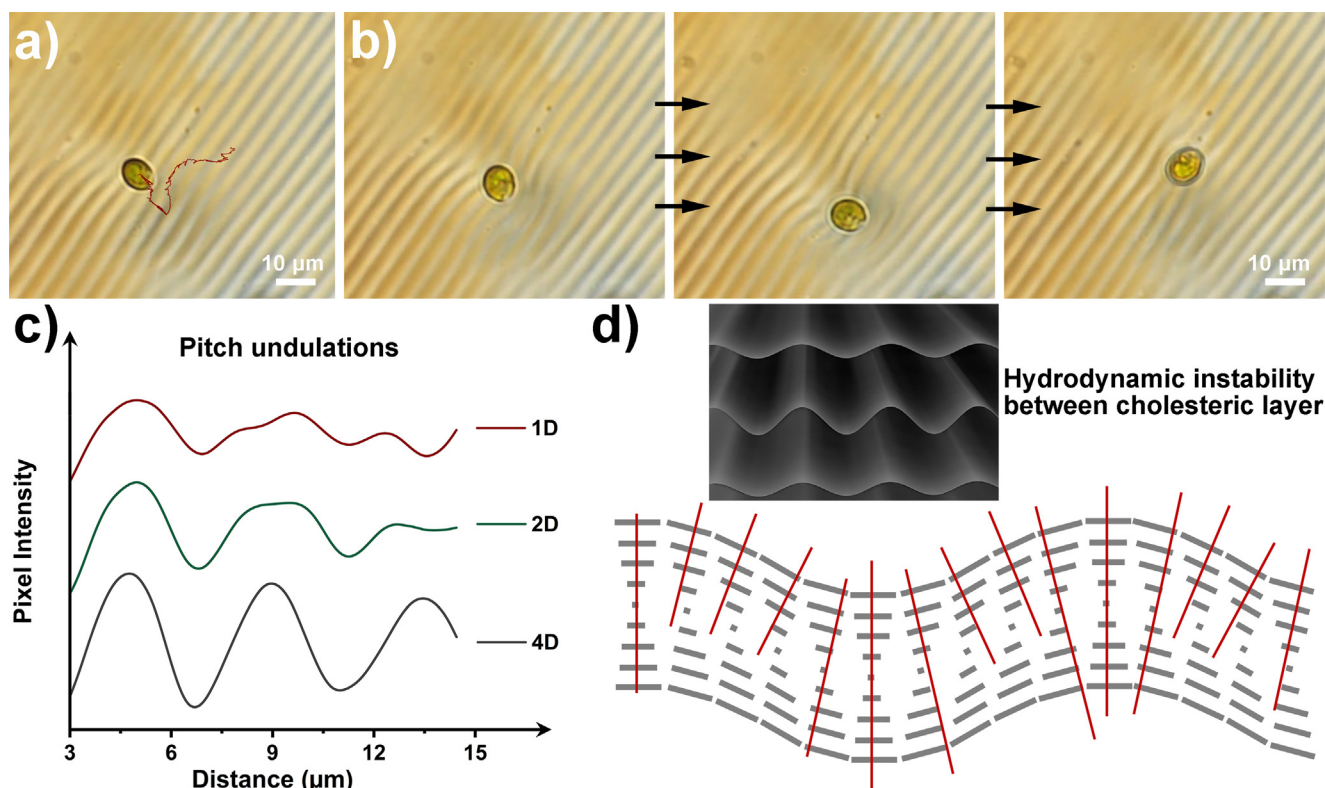


Fig. 3. (a) The swimming trajectory of an active CR in a purely cholesteric LC phase with high magnification and recorded during 30 s. (b) Series of magnified polarized microscopy images that focus on the hydrodynamic CR-LC interactions which lead to fluctuations in the surrounding cholesteric LC medium. Time interval, 4 s. (c) Pitch undulations in local cholesteric LC phase depending on the distance away from the moving CR, implying that the pitch perturbation intensity in local LC phase falls off in strength with the relative distance between CR and cholesteric fingerprint area. The measured distance between CR and cholesteric fingerprint area are one time (1D), two times (2D) and four times (4D) the diameter of the living cells, respectively. (d) Sketch of the Helfrich-Hurault instability of the cholesteric layers under hydrodynamic force and the corresponding helicoidal axis splay and layer undulation instability in local cholesteric LC medium near moving CR. The grey lines show the projection of the twisted director field onto the plane containing the splayed helicoidal axis (red lines). (For interpretation of the references to colour in this figure legend, the reader is referred to the web version of this article.)

strong to stretch the CNC assemblies and destabilize the cholesteric order, inducing local elastic stress and hydrodynamic instability in surrounding LC fluid. In other words, the beating flagella drive LC fluid flow in response to distortions in the helicoidal axis, with splay and bend distortions locally parallel and perpendicular to the director. Such deformations arise from the hydrodynamic stress within cholesteric layers, where the effective viscosity is much lower and creating a uniform conical tilt of the cholesteric director into the pitch direction [51]. If the activity is low, the cholesteric ordered CNC preserves its uniform static orientational ordering, whereas the activity increases above a critical threshold, the CNC orientation becomes progressively tilted due to the local hydrodynamic flow in surrounding LC. This phenomenon is analogous to the Helfrich-Hurault instability in passive cholesteric LC in response to extensional stress [52–54], namely, helicoidal axis splay and bend distortion of the director that is directed along the helicoidal axis (Fig. 3d). Finally, this hydrodynamic splay-bend mode in a cholesteric system was found to recover back to its initial state as the CR swims far away and displaying dynamic layer undulations.

We experimentally tracked the defect transition in surrounding cholesteric medium during the flagella beating process. Defects play a fundamental role in the description of ordered materials when a nonhomogeneous state cannot be eliminated by continuous variations of the order parameter, both from the viewpoint of passive and active matter. Defects in active LC, namely, disclinations and dislocations, are created by large enough activity and driven by active stresses [55]. The resulting active flow between

cholesteric layers yields layer undulation instability with the formation of line defect in cholesteric order, ascribing to the disclinations or dislocations in cholesteric layers. We present experimental results on the dynamic dislocation profile in the bulk of a layered cholesteric LC. Fig. 4a shows a sequence of images corresponding to flow-induced defect formation and recovery under the CR flagella beating process, which highlight the active cholesteric dislocations. From the ground state, an oriented fingerprint texture was observed indicating a uniform lying helix with the CNC nanorods perpendicularly anchored along the glass surface. With the CR approaching, the beating flagella stretched the CNC assemblies and distorted the local cholesteric texture, creating dynamic cholesteric dislocation (bifurcating lines) with a small Burgers vector ($b = p$, where p is the helical pitch), implying the splitting of χ dislocation into combination of two λ disclinations (Fig. 4b) [56]. When the beating stress on the local cholesteric assembly was reduced, namely, swimming far away from the beating-induced defect region, the dislocation recovered back to defect-free state which owing to the balance of elastic energy in the surrounding LC medium (Fig. S5). The obtained frustration of local fingerprint texture around the swimming CR was given by the mechanical stress in beating flagella, and dynamically resolved by the creation of line defect in the bulk phase. Therefore, we conclude that the swimming CR in a passive cholesteric LC fluid can induce layer undulations and hydrodynamic fluctuations in local surrounding medium, as well as creating reconfigurable defects during the flagella beating process, similar to the simulated active cholesteric LC counterpart.

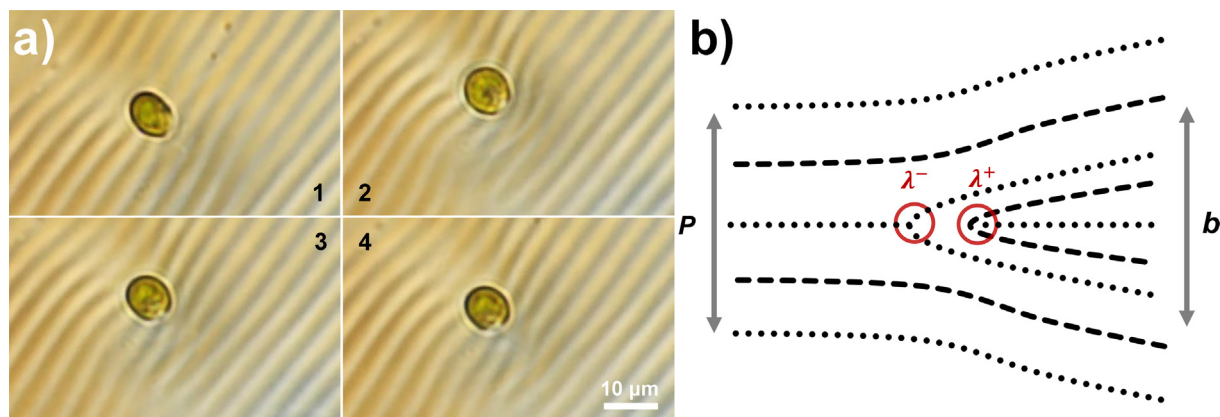


Fig. 4. (a) High magnified image sequence and relative scheme description that focus on the flow-induced dynamic dislocations in local fingerprint cholesteric LC. From 1 to 4 highlight the ground state, dynamic dislocations and recovery state in local cholesteric LC. (b) The resulting cholesteric dislocation comprises a pair of λ lines, with the director field that oriented out of the page is highlighted in dots. The red circles show the locations of the λ^+ and λ^- defects. (For interpretation of the references to colour in this figure legend, the reader is referred to the web version of this article.)

4. Conclusions

To summarize, here we describe a new kind of active matter composed of swimming CR microalgae dispersed in nontoxic lyotropic cholesteric CNC suspension. Owing to microalga's beating flagella, modulated locomotion behavior and hydrodynamic fluctuations take place in the fingerprint LC media. The self-propelled microalga can not only tune its swimming gait, direction, frequency, and speed through sensing the local environmental viscosity, but also display enough activity to overcome the stabilizing elastic force in surrounding LC matrix with random walk path. Owing to the beating flagella and micrometer-sized moving CR, the resulting active stress and disturbance flow stretch the CNCs assembly and generate layer undulations, helicoidal axis splay deformation and active line defects in surrounding LC medium. The demonstrated LC dispersed active matter, namely, internally driven active microalgae in anisotropic cholesteric CNC phase, is expected to open opportunities in the design of out-of-equilibrium functional biomechanical systems.

Declaration of Competing Interest

The authors declare that they have no known competing financial interests or personal relationships that could have appeared to influence the work reported in this paper.

Acknowledgement

This work was a part of the Academy of Finland's Flagship Programme under Projects No. 318890 and 318891 (Competence Center for Materials Bioeconomy, FinnCERES). G. C. acknowledges the financial support from the Novo Nordisk Foundation (Grant number: NNF20OC0064350). O.J.R. acknowledges support by the Canada Excellence Research Chair initiative (CERC-2018-00006), the Canada Foundation for Innovation (Project number 38623) and the European Research Council under the European Union's Horizon 2020 research and innovation program (ERC Advanced Grant Agreement No. 788489, "BioEiCell").

Appendix A. Supplementary material

Supplementary data to this article can be found online at <https://doi.org/10.1016/j.jcis.2022.05.012>.

References

- [1] M.C. Marchetti, J.F. Joanny, S. Ramaswamy, T.B. Liverpool, J. Prost, M. Rao, R.A. Simha, Hydrodynamics of soft active matter, *Rev. Mod. Phys.* 85 (3) (2013) 1143–1189.
- [2] S. Ramaswamy, The mechanics and statistics of active matter, *Annu. Rev. Condens. Matter Phys.* 1 (1) (2010) 323–345.
- [3] A.E. Patteson, A. Gopinath, P.E. Arratia, Active colloids in complex fluids, *Curr. Opin. Colloid Interface Sci.* 21 (2016) 86–96.
- [4] K. Copenhagen, R. Alert, N.S. Wingreen, J.W. Shaevitz, Topological defects promote layer formation in *Myxococcus xanthus* colonies, *Nat. Phys.* 17 (2) (2021) 211–215.
- [5] P.G. De Gennes, J. Prost, *The physics of liquid crystals*, Oxford University Press, 1993.
- [6] Y.-K. Kim, X. Wang, P. Mondkar, E. Bokusoglu, N.L. Abbott, Self-reporting and self-regulating liquid crystals, *Nature* 557 (7706) (2018) 539–544.
- [7] G. Chu, E. Zussman, From chaos to order: evaporative assembly and collective behavior in drying liquid crystal droplets, *J. Phys. Chem. Lett.* 9 (2018) 4795–4801.
- [8] P. Poulin, H. Stark, T.C. Lubensky, D.A. Weitz, Novel colloidal interactions in anisotropic fluids, *Science* 275 (5307) (1997) 1770–1773.
- [9] I. Musevic, M. Skarabot, Uros Tkalec, M. Ravnik, S. Zumer, Two-dimensional nematic colloidal crystals self-assembled by topological defects, *Science* 313 (5789) (2006) 954–958.
- [10] G. Chu, G. Vasilyev, R. Vilensky, M. Boaz, R. Zhang, P. Martin, N. Dahan, S. Deng, E. Zussman, Controlled assembly of nanocellulose-stabilized emulsions with periodic liquid crystal-in-liquid crystal organization, *Langmuir* 34 (44) (2018) 13263–13273.
- [11] C. Peng, T. Turiv, Y. Guo, Q.-H. Wei, O.D. Lavrentovich, Command of active matter by topological defects and patterns, *Science* 354 (6314) (2016) 882–885.
- [12] S. Zhou, A. Sokolov, O.D. Lavrentovich, I.S. Aranson, Living liquid crystals, *Proc. Natl. Acad. Sci.* 111 (4) (2014) 1265–1270.
- [13] C.J. Woolverton, E. Gustely, L. Li, O.D. Lavrentovich, Liquid crystal effects on bacterial viability, *Liq. Cryst.* 32 (4) (2005) 417–423.
- [14] P.C. Mushenheim, R.R. Trivedi, H.H. Tuson, D.B. Weibel, N.L. Abbott, Dynamic self-assembly of motile bacteria in liquid crystals, *Soft Matter* 10 (1) (2014) 88–95.
- [15] A. Patteson, A. Gopinath, M. Goulian, P. Arratia, Running and tumbling with *E. coli* in polymeric solutions, *Sci. Rep.* 5 (2015) 15761.
- [16] I.I. Smalyukh, J. Butler, J.D. ShROUT, M.R. Parsek, G.C. Wong, Elasticity-mediated nematiclike bacterial organization in model extracellular DNA matrix, *Phys. Rev. E* 78 (2008) 030701.
- [17] J.S. Guasto, K.A. Johnson, J.P. Gollub, Oscillatory flows induced by microorganisms swimming in two dimensions, *Phys. Rev. Lett.* 105 (2010) 168102.
- [18] R.J. Hickey, A.E. Pelling, Cellulose biomaterials for tissue engineering, *Front. Bioeng. Biotechnol.* 7 (2019) 45.
- [19] B.G. Rånby, A. Banderet, L.G. Sillén, Aqueous colloidal solutions of cellulose micelles, *Acta. Chem. Scand.* 3 (1949) 649–650.
- [20] B.G. Rånby, Fibrous macromolecular systems. Cellulose and muscle. The colloidal properties of cellulose micelles, *Discuss. Faraday Soc.* 11 (0) (1951) 158–164.
- [21] S. Beck-Candanedo, M. Roman, D.G. Gray, Effect of reaction conditions on the properties and behavior of wood cellulose nanocrystal suspensions, *Biomacromolecules* 6 (2) (2005) 1048–1054.
- [22] C. Calvino, N. Macke, R. Kato, S.J. Rowan, Development, processing and applications of bio-sourced cellulose nanocrystal composites, *Prog. Polym. Sci.* 103 (2020) 101221.

- [23] J.-F. Revol, H. Bradford, J. Giasson, R.H. Marchessault, D.G. Gray, Helicoidal self-ordering of cellulose microfibrils in aqueous suspension, *Int. J. Biol. Macromol.* 14 (3) (1992) 170–172.
- [24] L. Wang, A.M. Urbas, Q. Li, Nature-inspired emerging chiral liquid crystal nanostructures: from molecular self-assembly to DNA mesophase and nanocolloids, *Adv. Mater.* 32 (2020) 1801335.
- [25] J. Ma, Y. Yang, C. Valenzuela, X. Zhang, L. Wang, W. Feng, Mechanochromic, shape-programmable and self-healable cholesteric liquid crystal elastomers enabled by dynamic covalent boronic ester bonds, *Angew. Chem. Int. Ed.* 61 (9) (2022), <https://doi.org/10.1002/anie.v61.910.1002/anie.202116219>.
- [26] J. Yang, X. Zhang, X. Zhang, L. Wang, W. Feng, Q. Li, Beyond the visible: bioinspired infrared adaptive materials, *Adv. Mater.* 33 (2021) 2004754.
- [27] G. Chu, A. Camposeo, R. Vilensky, G. Vasilyev, P. Martin, D. Pisignano, E. Zussman, Printing flowers? Custom-tailored photonic cellulose films with engineered surface topography, *Matter* 1 (4) (2019) 988–1000.
- [28] G. Chu, F. Chen, B. Zhao, X. Zhang, E. Zussman, O.J. Rojas, Self-assembled nanorods and microspheres for functional photonics: retroreflector meets microlens array, *Adv. Opt. Mater.* 9 (9) (2021) 2002258, <https://doi.org/10.1002/adom.v9.910.1002/adom.202002258>.
- [29] S.N. Fernandes, P.L. Almeida, N. Monge, L.E. Aguirre, D. Reis, C.L. de Oliveira, A. M. Neto, P. Pieranski, M.H. Godinho, Mind the microgap in iridescent cellulose nanocrystal films, *Adv. Mater.* 29 (2017) 1603560.
- [30] P. Lv, X. Lu, L. Wang, W. Feng, Nanocellulose-based functional materials: from chiral photonics to soft actuator and energy storage, *Adv. Funct. Mater.* 31 (2021) 2104991.
- [31] J.A. Kelly, M. Giese, K.E. Shopsowitz, W.Y. Hamad, M.J. MacLachlan, The development of chiral nematic mesoporous materials, *Acc. Chem. Res.* 47 (4) (2014) 1088–1096.
- [32] K.E. Shopsowitz, H. Qi, W.Y. Hamad, M.J. MacLachlan, Free-standing mesoporous silica films with tunable chiral nematic structures, *Nature* 468 (7322) (2010) 422–425.
- [33] G. Chu, D. Qu, E. Zussman, Y. Xu, Ice-assisted assembly of liquid crystalline cellulose nanocrystals for preparing anisotropic aerogels with ordered structures, *Chem. Mater.* 29 (9) (2017) 3980–3988.
- [34] G. Chu, R. Vilensky, G. Vasilyev, S. Deng, D. Qu, Y. Xu, E. Zussman, Structural transition in liquid crystal bubbles generated from fluidic nanocellulose colloids, *Angew. Chem.* 129 (30) (2017) 8877–8881.
- [35] L. Bai, S. Huan, B. Zhao, Y.a. Zhu, J. Esquena, F. Chen, G. Gao, E. Zussman, G. Chu, O.J. Rojas, All-aqueous liquid crystal nanocellulose emulsions with permeable interfacial assembly, *ACS nano* 14 (10) (2020) 13380–13390.
- [36] G. Chu, G. Vasilyev, D. Qu, S. Deng, L. Bai, O.J. Rojas, E. Zussman, Structural arrest and phase transition in glassy nanocellulose colloids, *Langmuir* 36 (4) (2020) 979–985.
- [37] M. Zeng, D. King, D. Huang, C. Do, L. Wang, M. Chen, S. Lei, P. Lin, Y. Chen, Z. Cheng, Iridescence in nematics: Photonic liquid crystals of nanoplates in absence of long-range periodicity, *Proc. Natl. Acad. Sci.* 116 (2019) 18322–18327.
- [38] G. Chu, X. Wang, T. Chen, W. Xu, Y. Wang, H. Song, Y. Xu, Chiral electronic transitions of YVO₄: Eu³⁺ nanoparticles in cellulose based photonic materials with circularly polarized excitation, *J. Mater. Chem. C* 3 (2015) 3384–3390.
- [39] J. Majoinen, E. Kontturi, O. Ikkala, D.G. Gray, SEM imaging of chiral nematic films cast from cellulose nanocrystal suspensions, *Cellulose* 19 (5) (2012) 1599–1605.
- [40] S.A. Khadem, M. Bagnani, R. Mezzenga, A.D. Rey, Relaxation dynamics in bio-colloidal cholesteric liquid crystals confined to cylindrical geometry, *Nat. Commun.* 11 (2020) 4616.
- [41] N. Sueoka, Mitotic replication of deoxyribonucleic acid in *Chlamydomonas reinhardi*, *Proc. Natl. Acad. Sci. U.S.A.* 46 (1) (1960) 83–91.
- [42] P. Saha, V.A. Davis, Photonic properties and applications of cellulose nanocrystal films with planar anchoring, *ACS Appl. Nano Mater.* 1 (5) (2018) 2175–2183.
- [43] E.H. Harris, The *Chlamydomonas* Sourcebook: Introduction to *Chlamydomonas* and Its Laboratory Use, Academic Press, Volume 1, 2009.
- [44] D.B. Weibel, P. Garstecki, D. Ryan, W.R. DiLuzio, M. Mayer, J.E. Seto, G.M. Whitesides, Microoxen: microorganisms to move microscale loads, *Proc. Natl. Acad. Sci.* 102 (2005) 11963–11967.
- [45] B. Qin, A. Gopinath, J. Yang, J.P. Gollub, P.E. Arratia, Flagellar kinematics and swimming of algal cells in viscoelastic fluids, *Sci. Rep.* 5 (2015) 9190.
- [46] M. Polin, I. Tuval, K. Drescher, J.P. Gollub, R.E. Goldstein, *Chlamydomonas* swims with two “gears” in a eukaryotic version of run-and-tumble locomotion, *Science* 325 (5939) (2009) 487–490.
- [47] O.D. Lavrentovich, Active colloids in liquid crystals, *Curr. Opin. Colloid Interface Sci.* 21 (2016) 97–109.
- [48] J.C. Loudet, P. Hanusse, P. Poulin, Stokes Drag on a Sphere in a Nematic Liquid Crystal, *Science* 306 (2004) 1525–1525.
- [49] D. Marenduzzo, E. Orlandini, J. Yeomans, Permeative flows in cholesteric liquid crystals, *Phys. Rev. Lett.* 92 (2004) 188301.
- [50] A.D. Rey, Simple shear and small amplitude oscillatory rectilinear shear permeation flows of cholesteric liquid crystals, *J. Rheol.* 46 (1) (2002) 225–240.
- [51] C.A. Whitfield, T.C. Adhyapak, A. Tiribocchi, G.P. Alexander, D. Marenduzzo, S. Ramaswamy, Hydrodynamic instabilities in active cholesteric liquid crystals, *Eur. Phys. J. E: Soft Matter Biol. Phys.* 40 (2017) 50.
- [52] G. Chu, R. Vilensky, G. Vasilyev, P. Martin, R. Zhang, E. Zussman, Structure evolution and drying dynamics in sliding cholesteric cellulose nanocrystals, *J. Phys. Chem. Lett.* 9 (8) (2018) 1845–1851.
- [53] J.P. Hurault, Static distortions of a cholesteric planar structure induced by magnetic or AC electric fields, *J. Chem. Phys.* 59 (4) (1973) 2068–2075.
- [54] B. Senyuk, I.I. Smalyukh, O. Lavrentovich, Undulations of lamellar liquid crystals in cells with finite surface anchoring near and well above the threshold, *Phys. Rev. E* 74 (2006) 011712.
- [55] S.J. DeCamp, G.S. Redner, A. Baskaran, M.F. Hagan, Z. Dogic, Orientational order of motile defects in active nematics, *Nat. Mater.* 14 (11) (2015) 1110–1115.
- [56] O.D. Lavrentovich, M. Kleman, *Cholesteric Liquid Crystals: Defects and Topology, Chirality in Liquid Crystals*, Springer, in: H.-S. Kitzerow, C. Bahr (Eds.), *Partially Ordered Systems Chirality in Liquid Crystals*, Springer-Verlag, New York, 2001, pp. 115–158, https://doi.org/10.1007/0-387-21642-1_5.